Current distribution in a parallel configuration superconducting strip-line detector

A. Casaburi,[1] R. M. Heath,[1] M. G. Tanner,[1] R. Cristiano,[2] M. Ejrnaes,[2] C. Nappi,[2] and R. H. Hadfield[1]
[1]*School of Engineering, University of Glasgow, Glasgow G12 8LT, United Kingdom*
[2]*CNR—Istituto di Cibernetica "E. Caianiello," 80078 Pozzuoli, Italy*

(Received 11 April 2013; accepted 18 June 2013; published online 2 July 2013)

Superconducting detectors based on parallel microscopic strip-lines are promising candidates for single molecule detection in time-of-flight mass spectrometry. The device physics of this configuration is complex. In this letter, we employ nano-optical techniques to study the variation of current density, count rate, and pulse amplitude transversely across the parallel strip device. Using the phenomenological London theory, we are able to correlate our results to a non-uniform current distribution between the strips, governed by the London magnetic penetration depth. This fresh perspective convincingly explains anomalous behaviour in large area parallel superconducting strip-line detectors reported in previous studies. © *2013 AIP Publishing LLC*.
[http://dx.doi.org/10.1063/1.4813087]

Single-molecule detectors for time-of-flight mass spectrometry (TOF-MS) require the following characteristics: sub-nanosecond response time, low timing jitter, large sensitive area, and high efficiency when detecting heavy mass particles (>100 kDa). Superconducting strip-line detectors (SSLDs) have emerged as promising candidates for ultrafast detection of heavy single particles, as demonstrated in the first beam line test.[1] These devices were originally developed for the detection of single photons of $E < 1\,\mathrm{eV}$[2] and typically consist of 100 nm width and 5–10 nm thick niobium nitride (NbN) superconducting strip-lines cooled below the superconducting transition temperature (usually to $T \sim 4\,\mathrm{K}$) and biased just below the superconducting critical current. When a single infrared photon strikes the strip, a fast voltage pulse is triggered through supercurrent assisted hot-spot formation and can be recorded by room temperature electronics.[3] The same working principle can be applied to detect single molecules with $E \sim 20\,\mathrm{keV}$ in TOF-MS with superconducting strips of widths up to 1 μm and thicknesses between the range 10 –50 nm.[1,4] The response time of the device is limited by the strip-line kinetic inductance, L_k, which increases in proportion to the strip-line length.[5] Therefore, a "parallel" strip-line configuration is adopted to increase the coverage area whilst retaining an ultra-fast response.[6,7] This simple idea allows precise control of the kinetic inductance of strip-line elements, leading to the realization of an SSLD with a sensitive area up to $2 \times 2\,\mathrm{mm}^2$ with a sub-nanosecond response time.[4] In these large area SSLDs, a relatively low ratio of bias current to critical current ($I_B/I_C < 55\%$) is required to prevent device latching.[8] This bias current value is less than the threshold current required to induce the cascade switching of multiple strip-lines;[6] the device operates in the "single-strip switch regime."[9–11] In this regime, only the strip-line which has been struck switches partially into the normal state; the other parallel strips in the block remain completely superconducting. The current that was flowing in the impacted strip-line, will be diverted into the neighbouring parallel strips of the block, and only 0.01–1% of this current is diverted into the load impedance of the read-out circuit. However, because the strip-line cross section is large, the overall bias current is ~mA, thus the current diverted to the load (μA) is sufficient to register well distinguished pulses with a high signal-to-noise ratio.[4,7] In this regime, the strip-line does not recover its bias current after switching and the bias current is redistributed between the remaining superconducting strips.[10] This leads to variations in the efficiency during free running operation[4] and a spread in the pulse amplitude distribution.[11]

In this letter, we investigate the origin of the non-uniform current distribution among the strips during the biasing of the device, before any switching. In order to carry out this study, we fabricated an especially designed SSLD made of 6 parallel strip-lines having width of 1 μm, length of 200 μm, and spaced by 5 μm (pitch 6 μm) for a filling factor of 16.7% and an active area of $1.2\,\mathrm{mm}^2$ (see Figs. 1(a) and 1(b)). The starting point for the device was a 40 nm thick NbN film grown by DC magnetron reactive sputtering on a MgO substrate. The strip-line layout was created by electron beam lithography and reactive ion etching. Extra meanders made of 16 strips (8 each side) with width of 8 μm and spacing of 1 μm were patterned at the side of the 6 parallel strips to provide extra inductance in order to slow down the output pulses and to allow the pulse temporal profiles to be captured accurately with a 8 GHz bandwidth oscilloscope. Figs. 1(c) and 1(d) show the current-voltage characteristic measured at $T = 3.5\,\mathrm{K}$ and the resistance versus temperature curve for the patterned device, respectively. The device has a critical current of $I_C = 29.6\,\mathrm{mA}$ at 3.5 K and the critical temperature, $T_C = 15.6\,\mathrm{K}$. In this work, we employed an optical fiber-coupled miniature confocal microscope[11] integrated in a closed-cycle Pulse Tube (PT) refrigerator operating at $T = 3.5\,\mathrm{K}$.[12,13] The microscope optics are mounted on x,y, and z piezoelectric motors, enabling the optical spot to be precisely aligned and brought into focus on the device. Furthermore, a piezoelectric x-y scanner allows the optical spot to be translated across a 30 μm × 30 μm area with nanometre precision. The focussed optical spot (wavelength, $\lambda = 1550\,\mathrm{nm}$) on the device measures 1300 ± 360 nm (FWHM), with the PT

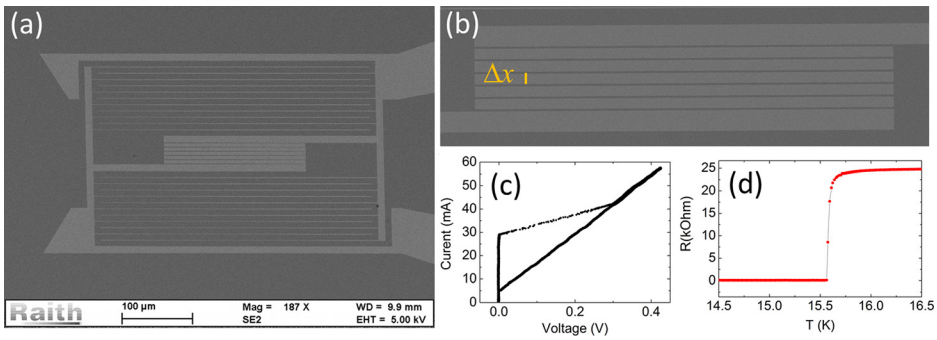

FIG. 1. (a) Scanning electron microscope (SEM) image of the whole SSLD; the darkest colour is the NbN. (b) SEM close-up of the 6 parallel strip-lines, with the spacing $\Delta x = 5\,\mu$m between strip-lines indicated. (c) Current–voltage characteristic of the SSLD measured at T = 3.5 K. (d) Resistance versus temperature curve of the SSLD.

cold head running. A 50 mW laser diode ($\lambda = 1550$ nm) and a fast electrical pulse generator were used to generate laser pulses having temporal width less than 400 ps and an energy per pulse ($E \sim 10$ MeV) sufficient to cause strip-line switching at a bias current as low as $I_b = 10$ mA ($\sim 0.3\, I_C$). This allowed us to drive a microscopic region of the strip out of equilibrium and nucleate a hotspot. We could then study the subsequent dynamics of the device. Current bias and signal pulse readout were performed using a bias tee. The signal pulses were amplified using two amplifiers in series with a total gain of 56 dB. The pulses were recorded on an 8 GHz bandwidth oscilloscope.

We firstly focused the laser beam on the NbN film by maximizing the intensity of reflected laser light (recorded on a conventional PIN diode). By scanning the stage motor over an area of $100 \times 500\ \mu m^2$, we recorded a reflected image of the device. This initial map gave us the coordinates of the strip-line positions. We then recorded a count rate map of the device, scanning the laser transversely across the strips, shown in Fig. 2(a).

The device was operated at a bias current of 15 mA ($\sim 0.5\, I_C$) and each line of the plot was obtained at fixed laser attenuation for values varied in the range 0 –10 dB. For each data point, 1000 laser pulses were delivered. Between consecutive laser pulses, the bias current was reset, by being switched off and increased back to 15 mA. The bias was reset after each laser pulse because we were specifically

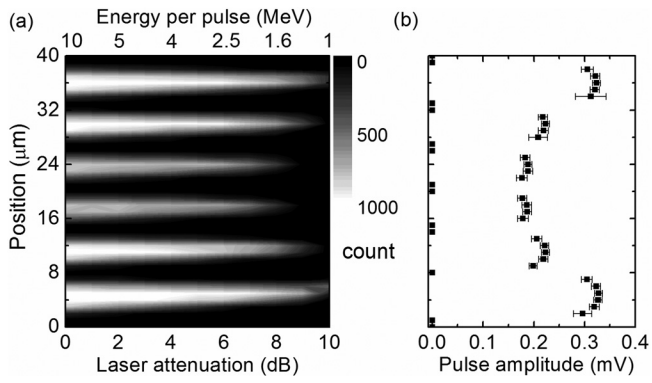

FIG. 2. (a) Contour plot of the count rate of the device measured as the number of the output voltage pulses counted for 1000 laser pulses delivered. (b) Maximum pulse amplitudes of the generated output pulses from the SSLD. Both sets of measurements (a) & (b) were performed by scanning the focussed laser spot transversely across the 6 strip-lines and operating the device at a bias current of 15 mA. In (a) each line scan was repeated by varying the laser attenuation in the range 0–10 dB (energy per pulse in the range 10-1 MeV) and in (b) attenuation was fixed at 5 dB (3.2 MeV). The scale and the caption of y axis are the same for (a) and (b).

interested in investigating the *initial* current distribution immediately after biasing. Moreover, as expected, no pulses were observed after the first; in the single strip switch regime, the strip-line does not recover the initial flowing bias current as already simulated in Ref. 9. It is possible to observe clearly in Fig. 2(a) that the count rate decreases from the outer strip-lines to the inner ones in a symmetric way. The same shape was observed for all the bias currents ranging between 13 mA and 23 mA. We attribute this to a non-uniform bias current distribution among strip-lines occurring just after biasing. Fig. 2(b) shows the maximum amplitude of the generated pulses. As in Fig. 2(a), the results of Fig. 2(b) were obtained by scanning the 5 dB attenuated laser in the same perpendicular direction across the strip-lines, whilst operating the device at a bias current of 15 mA. As shown, the maximum pulse amplitude decreases from the outer strip-lines toward the inner ones in a symmetric way, as observed for the count rate. A much smaller variation is observed within each strip-line from the middle toward the edges. This effect could be related to smaller overlapping (smaller photon flux) of the laser spot with the strips when the laser spot is moved toward edges. This results in a smaller hotspot size and the generation of output pulses with reduced amplitude. Moreover, we observed that the increase in the pulse amplitude is proportional to the increase in the total bias current, I_B; similarly, this variation is linear for each strip-line. As the maximum pulse amplitude increases linearly with increased flowing current in a single strip-line,[14,15] the observed linear trend implies that the ratio $I_i/I_B =$ constant as I_B varies, where I_i is the current flowing in i-th strip-line; i.e., the flowing current I_i increases linearly with increased I_B. Therefore, we conclude that there is a symmetrical and non-uniform current distribution among the parallel strip-lines after initial biasing and the ratio $I_i/I_B =$ constant, for each I_i, as I_B varies.

In order to explain this non-uniform current distribution among the strip-lines after biasing, we consider the London equation:[16]

$$\nabla^2 \mathbf{j} = \frac{1}{\lambda^2}\mathbf{j}, \tag{1}$$

with the hypothesis that well inside the thin strip-lines $j_x = j_z = 0$ and $j_y(x) = j(x) = j_y$, where j_x, j_y, and j_z are the Cartesian components of the current density vector $\mathbf{j}$ and λ is the effective magnetic penetration depth. The x component is oriented transverse to the strips. The last equality is valid for a strip-line width $w < \lambda$. In this regime, Eq. (1) becomes

$$\frac{\partial^2}{\partial_x^2} j(x) = \frac{1}{\lambda^2} j(x). \tag{2}$$

The discrete form of this expression for the different strip-lines can be written as $j_{i+1} - (2+a)j_i + j_{i-1} = 0$ $i = 2, 3 \ldots N-1$, where $a = \frac{\Delta x^2}{\lambda^2}$, Δx is the spacing between the strip-lines and j_i is the current density that is flowing in the i-th strip-line. Guided by our experimental observations and the symmetry of the device layout, we assume that the current in the first and last strip-lines is equal: $j_1 = j_N = j^*$. By solving the system with $N = 6$ for j_i/j^*, we obtain the solution with free parameter a,

$$\begin{aligned} \frac{j_1}{j^*} &= \frac{j_6}{j^*} = 1 \\ \frac{j_2}{j^*} &= \frac{j_5}{j^*} = \frac{1+a}{1+3a+a^2} \\ \frac{j_3}{j^*} &= \frac{j_4}{j^*} = \frac{1}{1+3a+a^2}. \end{aligned} \tag{3}$$

The values A_i, the maximum amplitude of the pulse generated by the i-th strip, were measured at the bias current of 23 mA in the middle each individual strip-line, where the count rate and the amplitude reach their maximum value. At that current, the pulse amplitude variation is less than 3% as the laser light attenuation is varied in the range 0-10 dB (this effect could be related to the complex dynamics involved in the generation of the hot spot by using an extended high energy laser pulse instead of a single photon). Therefore, we can assume $A_i/A^* = I_i/I^* = j_i/j^*$; the last equality is valid for uniform current distribution in the strip-lines (as assumed in Eq. (2)), where $A^* \equiv A_1 = A_6$ and $I^* \equiv I_1 = I_6$. For $\Delta x = 5\mu$m, the solution of Eq. (3) reproduces the A_i/A^* data (see Fig. 3) well, with the best fit value of $a = 0.239 \pm 0.002$ corresponding to a magnetic penetration depth of $\lambda = 10.2 \pm 0.2$ μm. This value should be compared with the London penetration depth λ_L obtained by measuring the fall-time, τ_{fall}, of the voltage pulses. In fact, τ_{fall} is given by the simple equation $\tau_{\text{fall}} = L_k/R_L$,[5] where R_L is the amplifier input impedance ($R_L = 50\,\Omega$). The kinetic inductance of the superconducting strip-lines can be written as $L_k = \mu_0 \lambda^2_L 2\, l/(wd)$, where μ_0 is the vacuum permeability constant and l, w, and d are the strip-line length, width, and thickness, respectively. The τ_{fall} is defined as the time constant of the exponential decay of the output pulse. We measured the average 90%–10% fall time, $\tau_{90\%-10\%}$, and then we used the formula $\tau_{\text{fall}} = \tau_{90\%-10\%}/2.197$, to infer τ_{fall}. The optical spot was directed at the same locations on the device where we measured the A_i. An average value of $\tau_{\text{fall}} = 371 \pm 16$ ps for the six strip-lines biased at 23 mA is obtained. This value was observed to be independent of the laser attenuation for each strip-line. By considering all the parts of the device, $d = 40 \pm 5$ nm and with $R_L = 50\ \Omega$ corresponding to the impedance of the electronic readout, we obtain $\lambda_L = 701 \pm 59$ nm. By using the corrected formula of the effective magnetic penetration depth[16] for magnetic field perpendicular to thin films ($d < \lambda_{\text{eff}}$), $\lambda_{\text{eff}} = \lambda^2_L/d = 12.2 \pm 3.6\,\mu$m, we obtain a value in agreement with that measured by fitting the pulse amplitudes with the London theoretical model. In obtaining this result, we disregarded the current dependence of the kinetic inductance.[15] From these measurements, it is possible to clearly understand the role played by λ_L in governing the temporal characteristics of the generated pulses (in particular, the fall time). Furthermore, we see that the effective magnetic penetration depth, corrected for the thickness of the superconducting films, together with the spacing between strip-lines, determines the bias current distribution among the parallel strip-lines after the initial biasing. Moreover, the fact that the current adheres to a distribution satisfying the London equation means that after each strip-line switching event the current will be *redistributed* among the remaining parallel strips in a non-trivial fashion $I_i/(N\text{-}1)$. The new current distribution satisfies the London theory and can be obtained by solving the discrete version of Eq. (3) with $I_i = 0$ or equal to a very small current value. The effects discussed are very important to consider when designing large area parallel SSLDs for TOF-MS experiments because a strong non uniform current distribution will affect the maximum critical current, the count rate, and the latching of the detector in the single strip-switch regime. Fig. 4 illustrates j_i/j^* calculated for a device with $N = 20$, $\Delta x = 1\,\mu$m, and $\lambda_{\text{eff}} = 8.13\,\mu$m ($a = 0.015$) identical parameters to the device used in Ref. 4. As can be seen from Fig. 4, the current distribution is strongly non uniform and this explains succinctly why the 2×2 mm^2 SSLD device reported in Ref. 4 (the largest area SSLD to date) did not show the expected count rate increase compared with the 1×1 mm^2 SSLD of Ref. 7. In

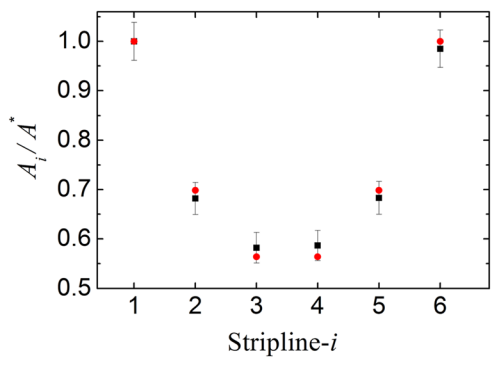

FIG. 3. The black squares are the ratio of the measured amplitudes A_i of pulses generated when the laser pulse strikes i-th strip-line and $A_1 = A^*$ of strip-line 1. The amplitudes were measured for laser attenuation of 5 dB (3.2 MeV) in the middle of the strip-lines. The red circles are the ratio of the current j_i flowing in i-th strip-line and $j_1 = j^*$ flowing in the strip-line 1 obtained by solving discrete version of Eq. (3) for $N = 6$ and $a = 0.239$.

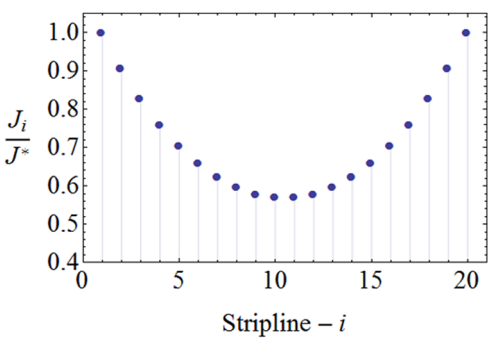

FIG. 4. Ratio of the current density flowing in the i-th strip-line (j_i) to that flowing strip-line 1 (j^*). These data were obtained by solving the discrete version of Eq. (3) for $N = 20$ and $a = 0.015$.

the strips in the central region, the current would be so low that the detection probability (count rate) could be close to 0 when the device is biased at $I_B/I_C = 0.52$. As a large part of the device is insensitive under these conditions, the overall count rate is reduced.

In conclusion, we have realized a carefully designed SSLD layout in parallel configuration and studied the non-uniform current distribution in the strips using a tightly focussed laser spot delivering energy of $\sim$10 MeV per pulse, equivalent to the impact of a molecular fragment in TOF-MS. By using the London phenomenological theory, we were able to explain our observations and reproduce the measured current flow in the strip-lines. The results of this experiment give an interesting insight into the role played by the London penetration depth for the current distribution and for the device physics of parallel SSLDs. This study represents an important step forward in the development of next generation parallel configuration designs with large active areas, for both SSLD for TOF-MS and SNSPDs for infrared single-photon detection.

We acknowledge support from the Royal Society of London, the Engineering and Physical Sciences Research Council, the US Air Force EOARD and EF7 E! Eurostars.

[1]K. Suzuki, S. Miki, S. Shiki, Z. Wang, and M. Ohkubo, Appl. Phys. Express **1**, 031702 (2008).
[2]G. N. Gol'tsman, O. Okunev, G. Chulkova, A. Lipatov, A. Semenov, K. Smirnov, B. Voronov, A. Dzardanov, C. Williams, and R. Sobolewski, Appl. Phys. Lett. **79**, 705 (2001).
[3]A. D. Semenov, G. N. Gol'tsman, and A. A. Korneev, Physica C **351**, 349 (2001).
[4]A. Casaburi, E. Esposito, M. Ejrnaes, K. Suzuki, M. Ohkubo, S. Pagano, and R. Cristiano, Supercond. Sci. Technol. **25**, 115004 (2012).
[5]A. J. Kerman, E. A. Dauler, W. E. Keicher, J. K. W. Yang, K. K. Berggren, G. N. Gol'tsman, and B. Voronov, Appl. Phys. Lett. **88**, 111116 (2006).
[6]M. Ejrnaes, R. Cristiano, O. Quaranta, S. Pagano, A. Gaggero, F. Mattioli, R. Leoni, B. Voronov, and G. N. Gol'tsman, Appl. Phys. Lett. **91**, 262509 (2007).
[7]A. Casaburi, N. Zen, K. Suzuki, M. Ejrnaes, S. Pagano, R. Cristiano, and M. Ohkubo, Appl. Phys. Lett. **94**, 212502 (2009).
[8]A. J. Kerman, J. K. W. Yang, R. J. Molnar, E. A. Dauler, and K. K. Berggren, Phys. Rev. B **79**, 10509 (2009).
[9]F. Marsili, D. Bitauld, A. Gaggero, S. Jahanmirinejad, R. Leoni, F. Mattioli, and A. Fiore, New J. Phys. **11**, 045022 (2009).
[10]A. Casaburi, *Superconducting Strip-Lines for Mass Spectrometry* (Lambert Academic Publishing, Saarbrücken, 2010).
[11]N. Zen, A. Casaburi, S. Shiki, K. Suzuki, M. Ejrnaes, R. Cristiano, and M. Ohkubo, Appl. Phys. Lett. **95**, 172508 (2009).
[12]J. A. O'Connor, M. G. Tanner, C. M. Natarajan, G. S. Buller, R. J. Warburton, S. Miki, Z. Wang, S. W. Nam, and R. H. Hadfield, Appl. Phys. Lett. **98**, 201116 (2011).
[13]M. G. Tanner, L. San Emeterio Alvarez, W. Jiang, R. J. Warburton, Z. H. Barber, and R. H. Hadfield, Nanotechnology **23**, 505201 (2012).
[14]M. Ejrnaes, A. Casaburi, O. Quaranta, S. Marchetti, A. Gaggero, F. Mattioli, R. Leoni, S. Pagano, and R. Cristiano, Supercond. Sci. Technol. **22**, 055006 (2009).
[15]P. Haas, A. Semenov, H. W. Hubers, J. Beyer, A. Kirste, A. Schurig, K. Il'in, M. Siegel, A. Engel, and A. Smirnov, IEEE Trans. Appl. Supercond. **17**, 298 (2007).
[16]M. Tinkham, *Introduction to Superconductivity* (Mc Graw-Hill, Inc., New York, 1996).